A NOVEL DUAL-BAND RECONFIGURABLE SQUARE-RING MICROSTRIP ANTENNA

M. A. Alkanhal and A. F. Sheta

Department of Electrical Engineering
King Saud University
P.O. Box 800, Riyadh 11421, Saudi Arabia

Abstract—A novel compact dual-band reconfigurable square-ring microstrip antenna is presented. The tuning is achieved using a single varactor diode connected to a small square patch attached to an inner corner of the square-ring. The square patch perturbs the symmetry and splits the two degenerate modes to create dual-band operation. The frequency ratio in the range of 1.04 to 1.4 can be achieved by the proper selection of the square patch size. The lower resonance frequency can be further decreased by loading the square patch at its corner by a reverse biased varactor diode. The diode has almost no effect on the upper resonance frequency. This technique is used to implement an electronically tunable dual-band antenna on FR4 material with $\varepsilon_r = 4.5$ and 1.5 mm thickness. The size of the ring, the square patch, and the varactor used, are selected to yield a fixed upper resonance frequency at about 1.93 GHz. The resulting lower resonance frequency is tuned from 1.37 to 1.7 GHz in the voltage range from 0 to 30 V, respectively. The measurements agree well with simulation results.

1. INTRODUCTION

Microstrip antennas are now extensively used in many applications such as mobile and satellite communications due to their compactness, lightweight, low profile and conformability to any structure [1]. Microstrip antenna is, basically, a resonant structure. Therefore, conventional microstrip antennas such as rectangular, circular, and triangular, patches, when operating at their fundamental mode, one of the dimensions is about half the operating wavelength. The size of these structures is large and unsuitable to be used in many applications, especially at the lower microwave range. Various techniques have been

developed to reduce the size of conventional structures. One of the techniques is to cut slits or slots on the basic shapes which will result in new compact geometries like slotted L-shaped and ring microstrip antennas. The main disadvantage of the resulting compact structures is the associated bandwidth reduction. However, bandwidth can be increased by adding lossy elements, which affect the efficiency of the antenna. One possible solution to avoid the use of lossy elements is the use of tunable or reconfigurable antenna concept [2–4]. In this case the small size antenna would not cover all bands simultaneously, but provides narrower instantaneous bandwidths at higher efficiency than conventional antennas.

Tuning technique can be performed either mechanically by inserting shorting posts and stubs [5] or electronically by using varactor diodes or switching diodes. Varactor based tunable antennas have recently been studied in many configurations [6–10]. In [6], a half wave microstrip antenna is loaded by two varactor diodes at the antenna edges that retain its symmetry and minimize cross-polarized radiation. A 30% tuning range has been reported. More size reduction is achieved in PIFA configuration by terminating one of the edges by a shorting post and loading the other by a varactor diode [7]. Tuning bandwidth of the order of 50% is achieved by dividing a PIFA antenna into two sections where two varactor tuning diodes are loaded so they connect the two sections electronically together [8]. Tunable slot antennas have been recently proposed for dual-band operation [9, 10]. The two bands can be controlled individually [10] using two varactors appropriately located along the slot and biased by two individual biasing circuits. PIN diode switched tunable antennas have also been studied as a multi-band solution [11–13].

In this paper we propose a new square-ring antenna with tunable dual-band operation. Dual-band operation has been demonstrated using rectangular microstrip patch with square slot [14, 15] by exciting the two modes TM_{10} and TM_{01}. The resonance frequencies of the two modes are chosen by the proper selection of the rectangular dimensions. Analysis of conventional and double layer square ring antenna can be found in [16]. In our case, the tuning is achieved by loading the square ring with a square patch perturbation at an inner corner and then attaching a varactor diode at the free corner of the patch. The square patch perturbation splits the degenerate modes to loaded and unloaded modes and the ring performs dual-mode resonance at two different frequencies. The antenna is fed using coupled lines as shown in Fig. 1. Using this type of excitation, a thin ring strip width can be used and matching the antenna at both bands can be obtained in the entire tuning range. The effect of the square patch perturbation
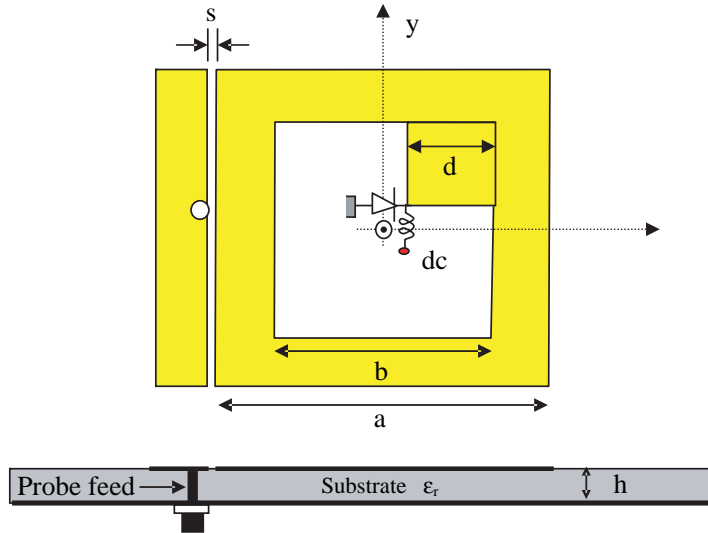
Figure 1. Geometry of tunable square-ring microstrip antenna.

on the ring is presented in the next section. Moreover, the effect of loading the square patch by a varactor diode is described in Section 3. Simulations and experimental results are given in Section 4 followed by conclusions in Section 5.

2. EFFECT OF THE SQUARE PATCH ATTACHED TO AN INNER CORNER

The square-ring microstrip antenna is obtained from the square patch by cutting a square slot at its center. In this case the resonance frequency of the patch decreases with an increase of the inner side of the slot, and reduces by, approximately, a factor of 2 when a thin strip width is used. The antenna size becomes approximately $\lambda/4 \times \lambda/4$ at the resonance of the dominant mode.

The proposed loaded square-ring microstrip antenna is shown in Fig. 1. The square-ring microstrip patch, has an inner side length b and outer side length of a. A square patch of side d is attached to an inner corner of the ring. The antenna is printed on FR4 substrate with dielectric constant 4.5 and thickness 1.5 mm. The tuning circuit, the varactor and its biasing circuit, are implemented at the corner of the perturbation. It has been reported that $50\,\Omega$ impedance matching could be achieved using direct probe feeding inside the ring strip for

wide strip width [12]. This will limit the advantage of the ring as a
compact antenna. Moreover, especially in our case, the flexibility of
the structure in tuning over a wide band will be limited. For this
reason, a probe excitation connected to air coupled line, as shown
in Fig. 1, is proposed. The air coupling is mainly depends on the
separation distance s. This excitation technique enables good matching
in the entire tuning range. Moreover, coupling capacitors that perform
isolation between the dc bias and the probe are no longer needed. The
ring size parameters $a = 26$ mm, $b = 20$ mm, $s = 0.2$ mm are used for
this analysis. For no perturbation the dominant excited mode is similar
to the TM_{11} mode in the annular ring antenna and is degenerate.
The resonant wavelength for this mode is nearly equal to the average
circumference of the ring. In this case the resonance frequency can be
approximated by

$$f_r = \frac{300}{L_{av}\sqrt{\varepsilon_{eff}}} \quad \text{(GHz)} \tag{1}$$

where, L_{av} is the average circumference $(a + b)/2$ in mm and ε_{eff} is
the effective relative dielectric constant of the strip ring.

This approximation is very accurate for narrow strip widths. For
the analyzed ring the strip width is 3 mm and the average circumference
is 92 mm. The resonance frequency from Eq. (1) is 1.75 GHz. The
resonance frequency of the ring estimated from IE3D is 1.81 GHz. The
percentage error is about 3.5%. This error reduces to 0.8% for 1 mm
strip width.

Introducing a square patch at the corner splits the degenerate
modes into two modes with two different resonant frequencies. Fig. 2
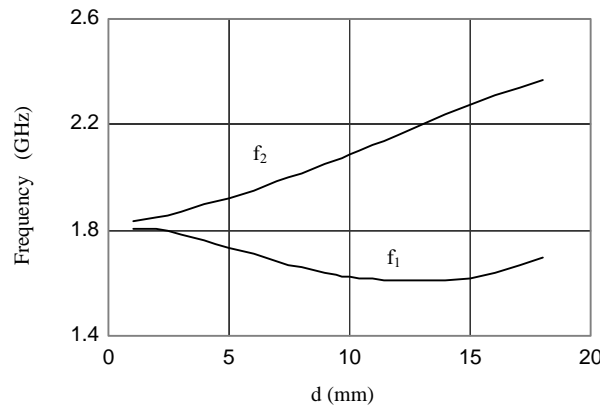

Figure 2. Effect of perturbation patch dimension d on the resonance
frequency of the split modes.
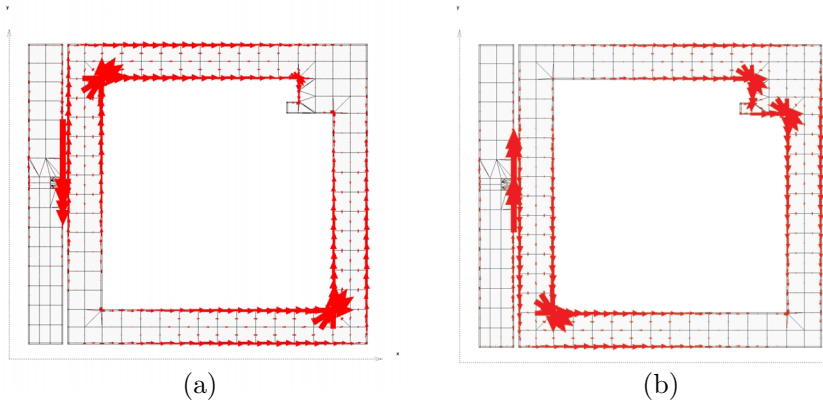
(a)   (b)

Figure 3. The current distribution of a square ring antenna loaded by a square patch of length $d = 3$ mm. (a) mode resonates at 1.78 GHz. (b) mode resonates at 1.88 GHz.

shows the effect of the size of the square patch d on the two resonance frequencies; the lower f_1, and the upper f_2. With increasing the perturbation patch size d, the upper frequency f_2 increases and the lower frequency f_1 decreases until d is about 14 mm, where the two frequencies both increase. Approximately, the structure above this value is no longer behaves as a square ring loaded by a square patch, rather it resembles a square patch loaded by L-slot.

The best way to explain the effect of the square patch length d on modes resonance frequencies is from the current distribution on the ring. Figs. 3a and 3b show the current distribution of the two modes at their resonance frequencies f_1 and f_2 for a square patch of side 3 mm. At the diagonal of the ring where the square patch exists, the mode of lower resonance frequency has a magnetic wall, while the mode of higher resonance frequency has an electric wall. The effective length of the ring for the mode having a magnetic wall increases as the square patch length d increases, and the square patch behaves as a stub at the end of the line. However, when an electric wall exists at the diagonal, the average current path will decrease and the ring effective length for such mode decreases and hence the resonance frequency increases with d. The ratio f_2/f_1 increases for increasing d and varies from about 1.014 for $d = 1$ mm to 1.39 for $d = 14$ mm. Fig. 4 shows the reflection coefficient S_{11} for various values of the perturbation size d. Good matching is achieved for almost all values of d.

The effect of the perturbation on the radiation pattern is also investigated using IE3D by plotting the radiation patterns with and
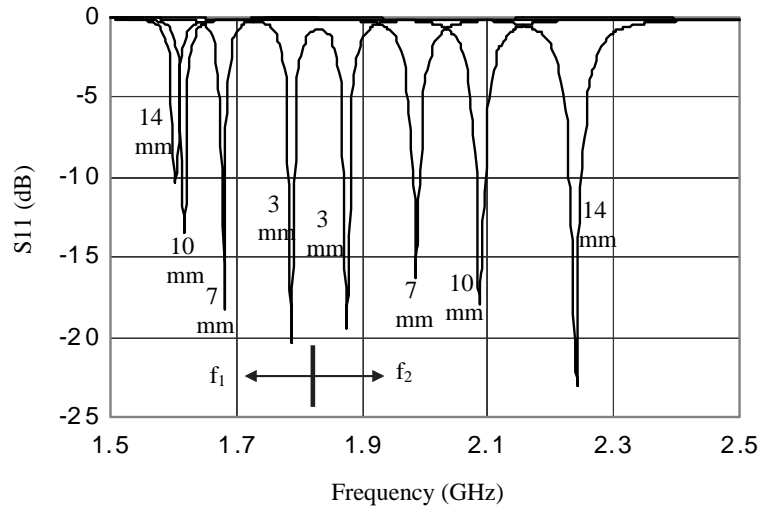
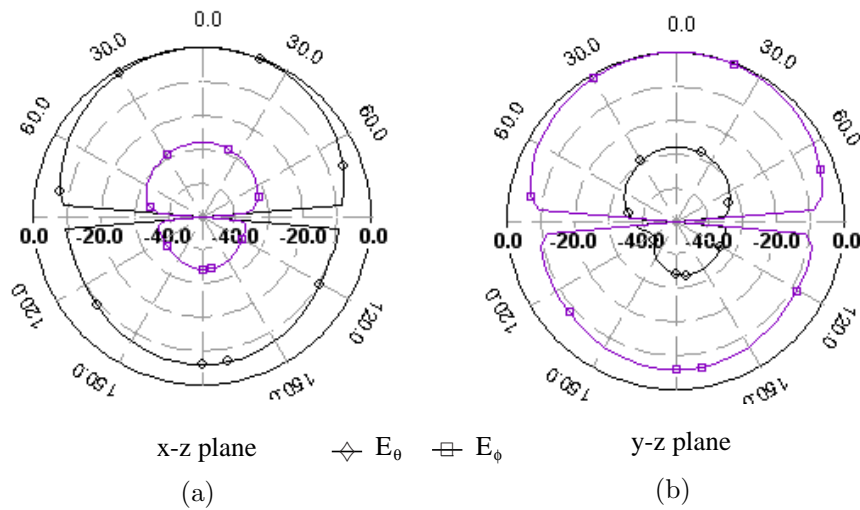**Figure 4.** Effect of the perturbation patch dimension d on the resonance frequencies f_1 and f_2.

Figure 5. Radiation pattern of the square-ring without perturbation at 1.81 GHz. (a) x-z plane. (b) y-z plane.

Figure 6. Radiation pattern of the square-ring with perturbation at 1.78 GHz. (a) x-z plane. (b) y-z plane.

without the square patch of size $d = 3\,\text{mm}$. A finite ground plane substrate of size $66 \times 66\,\text{mm}^2$ is used in the simulation. Fig. 5 shows the radiation pattern without the perturbation at the resonance frequency 1.81 GHz. Cross polarization less than $-27\,\text{dB}$ is observed in both x-z and y-z planes. The estimated gain and directivity are 1.3 and 5.3 dB, respectively. However, the perturbation increases the level of cross polarization, to about $-2\,\text{dB}$ in the same planes for both modes as shown in Figs. 6, and 7. The level of cross polarization can be reduced using appropriate perturbation instead of the square patch such as a thin stub. The gain and the directivity at the lower frequency $f_1 = 1.78\,\text{GHz}$ are almost the same as in the case of square ring without perturbation except of the shift in the plane of maximum power. Little increase in the gain and directivity is observed at $f_2 = 1.88\,\text{GHz}$ with a shift in the plane of maximum power.

3. EFFECT OF VARACTOR DIODE LOADING

The square ring loaded by a square patch at a corner is now loaded by a varactor diode connected at the free corner, of the square patch, as shown in Fig. 1. The current distribution shown in Fig. 3 indicates that at the diagonal of the ring where a square patch is loaded, one of the split modes has a magnetic wall and the other has an electric wall. Therefore, at the corner of the square, where the varactor is connected to the patch, the mode having an electric wall is, almost, not affected
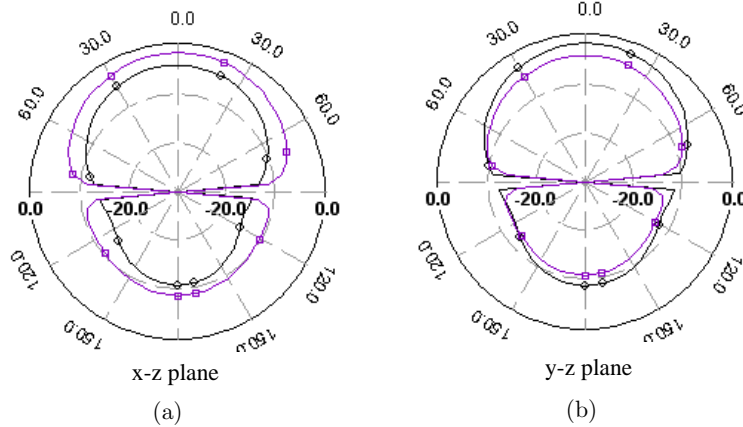
x-z plane

(a)

y-z plane

(b)

Figure 7. Radiation pattern of the square-ring with perturbation at 1.88 GHz. (a) x-z plane. (b) y-z plane.

by such loading. The field distribution of this mode doesn't change too much with the reverse bias voltage. Therefore, the resonance frequency f_2 is stays almost constant and independent of the varactor loading and can be fixed only by the size of the patch d. The effect of the varactor can be analyzed using IE3D by replacing the varactor by its model. A simple RF varactor model under reverse bias is shown in Fig. 8. The reactive components C_P and L_P model the packaging effect, while the C_J and R_S model the junction capacitance and the series resistance, respectively. For accurate analysis, the equivalent circuit parameters of the varactor should be considered. These parameters depend on the varactor type and the frequency of operation. The analysis carried out here is based on ideal varactor to study the effect of capacitance change on the frequency f_1. Accurate estimation of f_1 can be obtained for a particular device by introducing the equivalent circuit parameters as presented in the next section. The capacitance loading effect is studied
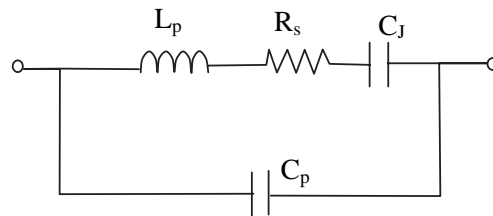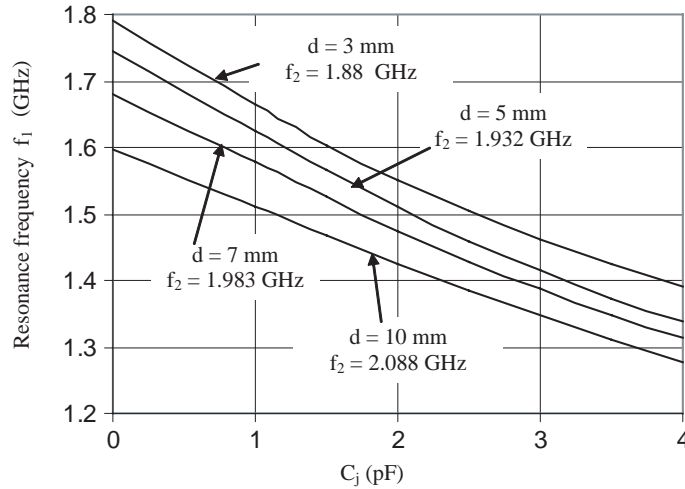

Figure 8. A simple varactor model.

Figure 9. Variation of the lower resonance frequency f_1 against junction capacitance (capacitance of a varactor diode under reverse bias located at the edge of the square patch as shown in Fig. 10) for different perturbation size d.

for capacitance change from 0 to 4 pF. These values are, practically, available at the lower microwave range. Fig. 9 shows the variation of f_1 with the loading capacitance C. The figure shows that the antenna can be tuned in a wide range. The upper frequency f_2 is defined by the square patch size d, while the lower resonance frequency f_1 is determined by the capacitance that, mainly, represents the junction capacitance of the varactor diode under a specified reverse voltage.

4. SIMULATION AND EXPERIMENTAL RESULTS OF TUNABLE DUAL-BAND ANTENNA

The tunable antenna analyzed in the previous sections is implemented with its tuning circuit on FR4 substrate with the same dimensions described in Section 2. A square patch perturbation of side length d of 3 mm is considered. In this case the upper resonance frequency f_2 is fixed at 1.88 GHz, while the lower resonance frequency is controlled electronically using a varactor diode. The diode used in our experiment is the SMTD3001 from Metelics Corp. The varactor's capacitance varies from 2.2 to 0.5 pF as the bias voltage is increased from 0 to 30 V as shown in Fig. 10. For ideal varactor capacitance equivalence, the expected frequency f_1, as given in Fig. 9, varies from 1.53 GHz (at
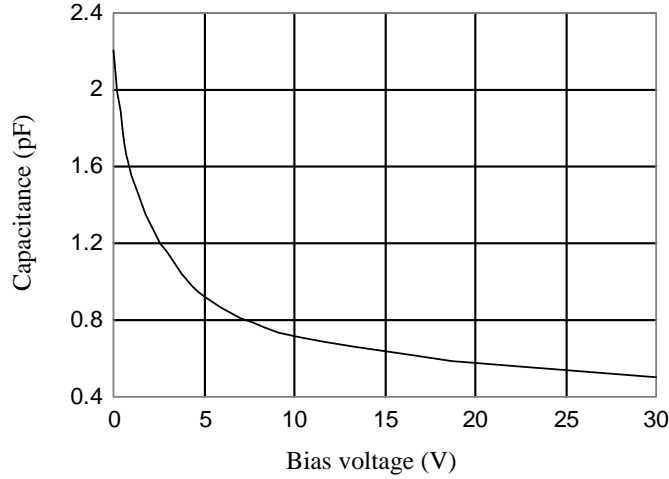
Figure 10. Typical capacitance of a SMTD3001 varactor (from Metelics Corp.) as a function of its bias voltage.

0 V) to 1.73 GHz (at 30 V). This tuning range is modified by taking into account the parasitic parameters effect. The typical values of the package parasitic parameters from the varactor data sheet are $L_P = 2$ nH and $C_P = 0.1$ pF. The series resistance has no effect on the resonance frequency f_1. The simulated S_{11}, calculated using IE3D, for different bias voltage is presented in Fig. 11. The package parasitic parameters are included and the series resistance of $0.7\,\Omega$ is also added to the model. The simulation results indicate that good simultaneous impedance match at both bands in the entire tuning range is obtained. The simulation shows that by increasing the dc bias from 0 to 30 V, the frequency of the first resonance f_1 increased from 1.378 to 1.69 GHz. As expected, a very little change in the upper frequency f_2, from 1.88 at 0 V to 1.884 at 30 V, is observed. It has to be noted that, the effect of the parasitic parameters is significant and could not be neglected and the estimation accuracy depends on how accurate the model is. The measured S_{11} of this antenna for different values of bias voltage is shown in Fig. 12. Good simultaneous impedance match at both bands in the entire tuning range is also observed. By changing the bias voltage from 0.5 to 3 V, the frequency f_1 can be tuned from 1.45 to 1.57 GHz. This means that, the tunable fractional bandwidth in this voltage change is about 6.6%. This bandwidth is suitable for almost all wireless mobile applications, where the available battery voltage is 3 V. Good agreement between the simulated and measured results can
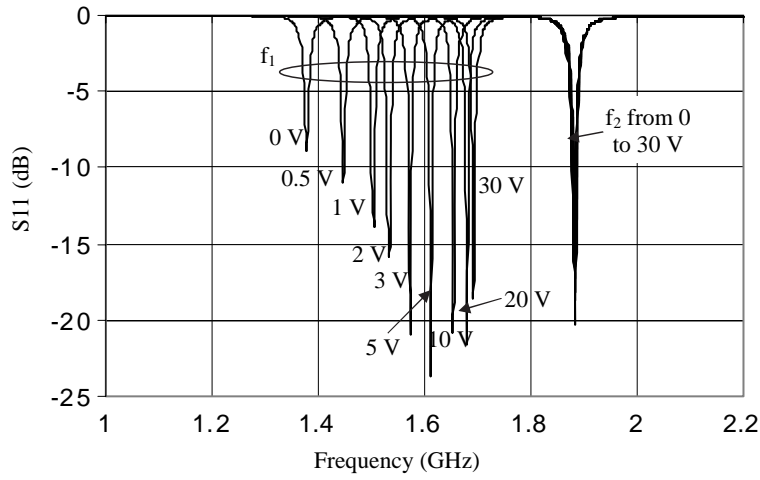
Figure 11. Simulation results of the tunable dual-band square-ring antenna for a voltage change from 0 to 30 V.
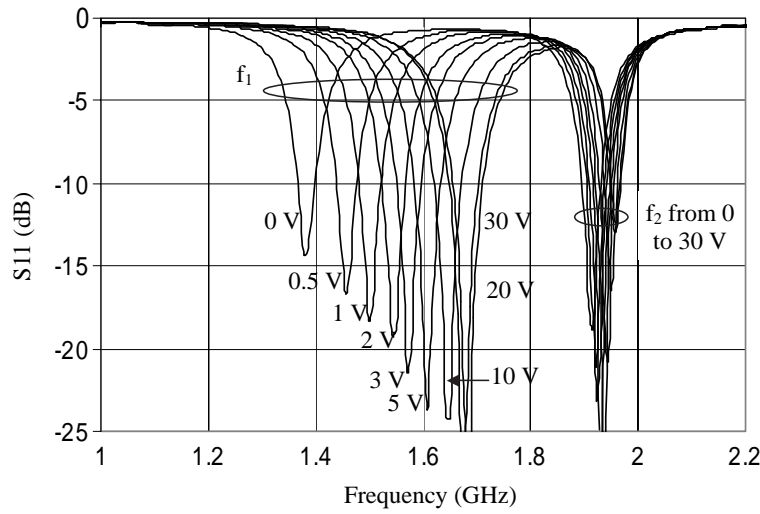

Figure 12. Measurements of the tunable dual-band square-ring antenna for a voltage change from 0 to 30 V.

be observed from the shown figures. Little decrease in gain is expected at the first mode due to the restraince of the varactor and tuning to the lower resonance frequency. However, the gain of the second (unloaded) mode remains, approximately, unchanged.

5. CONCLUSIONS

A novel compact dual-band tunable square-ring microstrip antenna is proposed in this paper. The dual-band operation is the result of splitting the degenerate modes by loading the square-ring by a perturbing square patch attached to an inner corner of the ring. The frequency ratio in the range of 1.04 to 1.4 is achieved by the prober selection of the square patch size. The mode of lower resonance frequency has a magnetic wall at the diagonal where the square patch attached, while the mode of higher resonance frequency has an electric wall at the same diagonal. The lower resonance frequency is, therefore, tuned by a varactor attached to the free corner of the square patch, while the upper resonance frequency remains fixed. An electronically tunable dual-band antenna was designed and implemented on FR4 material with $\varepsilon_r = 4.5$ and $1.5\,$mm thickness. The lower resonance frequency is tuned from 1.37 to 1.69 GHz for a voltage change from 0 to 30 V, while the upper resonance frequency has a little variation about 1.93 GHz. Simulations and experimental results showed good agreement. The tunable bandwidth in the voltage range from 0 to 3 V, is more than 8% which is suitable for almost all wireless handset mobile applications.

ACKNOWLEDGMENT

REFERENCES

1. Garg, R., P. Bhartia, I. Bahl, and A. Ittipiboon, *Microstrip Antenna Design Handbook*, Artech House, Boston, USA, 2001.
2. Aberle, J. T., S. H. Oh, D. T. Auckland, and S. D. Rogers, "Reconfigurable antennas for portable wireless devices," *IEEE Antennas and Propagation Magazine*, Vol. 45, No. 6, 148–158, December 2003.
3. Yang, X. S., B. Z. Wang, and H. L. Liu, "Reconfigurable Yagi patch array by utilizing odd-even-mode method," *Journal of*

Electromagnetic Waves and Applications, Vol. 20, No. 13, 1725–1738, 2006.

4. Shynu, S. V., G. Augustin, C. K. Aanandan, P. Mohanan, and K. Vasudevan, "Design of compact reconfigurable dual frequency microstrip antennas using varactor diodes," *Progress In Electromagnetics Research*, PIER 60, 197–205, 2006.

5. Mahmoud, S. F. and A. F. Sheta, "Cavity mode analysis for a rectangular patch with a shorting pin," *Journal of Electromagnetic Waves and Applications*, Vol. 20, No. 14, 2013–2025, 2006.

6. Bahartia, P. and Bahl, "Frequency agile microstrip antenna," *Microwave Journal*, Vol. 25, No. 10, 67–70, Oct. 1982.

7. Panayi, P. K., M. O. Al-Nuaimi, and L. P. Ivrissimtzis, "Tuning techniques for planar inverted-F antenna," *Electron. Lett.*, Vol. 37, No. 16, 1003–1004, 2001.

8. Virga, K. L. and Y. R. Samii, "Low-profile enhanced-bandwidth PIFA antennas for wireless communications packaging," *IEEE Trans. Microwave Theory Tech.*, Vol. 45, 1879–1888, October 1997.

9. Behdad, N. and K. Sarabandi, "A varactor-tuned dual-band slot antenna," *IEEE Trans. Antennas Propagat.*, Vol. 54, 401–408, February 2006.

10. Behdad, N. and K. Sarabandi, "Dual-band reconfigurable antenna with a very wide tenability range," *IEEE Trans. Antennas Propagat.*, Vol. 54, 409–416, February 2006.

11. Okabe, H. and K. Takei, "Tunable antenna system for 1.9 GHz PCS handsets," *Proc. IEEE AP-Symp.*, 166–169, 2001.

12. Karmakar, N. C., "Shorting strap tunable stacked patch PIFA," *IEEE Trans. Antennas Propagat.*, Vol. 52, 2877–2884, November 2004.

13. Peroulis, D., K. Sarabandi, and L. Katehi, "Design of reconfigurable slot antennas," *IEEE Trans. Antennas Propagat.*, Vol. 53, 645–654, February 2005.

14. Chen, W. S., "Single-feed dual-frequency rectangular microstrip antenna with square slot," *Electron. Lett.*, Vol. 34, 231–232, 1998.

15. Eldek, A. A. A. Z. Elsherbeni, and C. E. Smith, "Square slot antenna for dual wideband wireless communication systems," *Journal of Electromagnetic Waves and Applications*, Vol. 19, No. 12, 1571–1581, 2005.

16. Bafrooei, P. M. and and L. Shafai, "Characteristics of single- and Double layer microstrip square-ring antennas," *IEEE Trans. Antennas and Propagation*, Vol. 47, 1633–1639, October 1999.